Analysis of Battery Consumption in the Delivery Robot with 2 Brushed DC Motor

Muhammad Daffa Fadhlurrahman[1] and Anugerah Wibisana[1]

[1]Jurusan Teknik Elektro, Prodi Teknik Rekayasa Robotika, Politeknik Negeri Batam, Batam, Indonesia

Email: mhddaffa04@gmail.com

Received on dd-mm-yyyy | *Revised on dd-mm-yyyy* | *Accepted on dd-mm-yyyy*

Abstract— **This study evaluates the electrical performance and energy consumption of a delivery robot equipped with two brushed DC motors. The analysis focuses on how variations in motor speed, ranging from 1 to 5 RPS, affect battery endurance under a constant load of 8 kg. Data collection was performed using a PZEM-017 sensor integrated with an ESP32 microcontroller, allowing for real-time monitoring and cloud-based data logging via a MySQL database. The results indicate that increasing the RPS significantly raises the current draw, with power consumption escalating from 27.91 W at 1 RPS to 103.50 W at 5 RPS. Consequently, the battery usage time for a 4.5 Ah capacity decreased drastically from 234 minutes to 58 minutes at maximum stress. Furthermore, the study identifies a non-linear relationship between speed and energy depletion. These findings provide critical insights for optimizing power management and trajectory planning in autonomous mobile delivery robots.**

Keywords: Battery consumption, Brushed DC motor, Delivery robot, Energy efficiency, RPS variations.

I. INTRODUCTION

The rapid development of autonomous delivery robots has created new opportunities in logistics, healthcare, and service industries [1], [2]. These robots are commonly used for transporting goods in indoor environments such as hospitals, campuses, and warehouses [3], [4]. One of the most critical factors affecting the performance of delivery robots is battery energy consumption, which directly determines operating time, efficiency, and reliability [5], [6].

Most delivery robots use DC motors for mobility due to their simplicity, low cost, and ease of control [7]. However, brushed DC motors tend to consume significant electrical power, especially under heavy loads or uneven terrain [8]. Inefficient energy usage can reduce the robot's operational time and increase maintenance costs [9]. Therefore, analyzing battery energy consumption is essential for optimizing robot design and improving energy efficiency [10].

This study focuses on a delivery robot powered by a dual-battery configuration consisting of two 11.1 V Lithium Polymer (LiPo) batteries connected in series to provide a nominal voltage of 22.2 V. The robot is driven by two brushed DC motors and controlled by an ESP32 microcontroller. A PZEM-017 DC power monitoring module is employed to acquire real-time measurements of voltage (V), current (I), power (P), and energy consumption (E) from the battery system [11]. The collected data are transmitted to a local server using HTTP POST requests and stored in a MySQL database within a XAMPP environment, enabling reliable local data logging and post-experimental analysis.

In addition, previous studies have shown that the integration of intelligent sensing and monitoring approaches can enhance the operational safety and performance of autonomous robotic systems in indoor environments [12]. Furthermore, the use of PZEM-017 sensors has been proven effective for accurate monitoring of electrical parameters such as voltage, current, and power in energy monitoring applications [13]. Reliable data communication using RS485-based networks has also been widely adopted in industrial and robotic monitoring systems due to its robustness and stability [14]. Moreover, real-time battery monitoring systems play a crucial role in improving energy efficiency and extending the operational endurance of mobile robots [15].

The objective of this research is to evaluate the electrical performance and energy consumption characteristics of a delivery robot powered by a 22.2 V series battery system during operation. This study analyzes the relationship between motor load variations, represented by changes in rotational speed (RPS), and the resulting power and energy consumption. In addition, the battery usage efficiency and the reliability of a local database–based data logging system are evaluated to support accurate and continuous monitoring of the robot's energy usage.

II. METHOD

The object of this research is a power system consisting of two 11.1 V 3S Lithium Polymer (LiPo) batteries connected in series, providing a total nominal voltage of 22.2 V (equivalent to a 6-cell configuration), which is implemented in a delivery robot driven by two brushed DC motors. The measured variables include voltage, current, power, and energy consumption obtained from the battery system and monitored in real time.

This research includes motor rotational speed testing expressed in Revolutions Per Second (RPS), power consumption testing under payload variations, electrical power calculation, battery capacity estimation, and battery operational usage time analysis. In this study, motor rotational speed (RPS) refers to the relative motor operating speed level applied through the motor control system and is used to represent different motor operating conditions, rather than direct encoder-based measurements of shaft rotation. The motor rotational speed is evaluated at different RPS levels to analyze its effect on electrical power consumption and battery performance.

Data from these experiments are recorded and analyzed to evaluate the efficiency, stability, and overall performance of the battery system under various operating conditions. The results are then used to determine optimal operating strategies and to ensure reliable operation of the delivery robot during typical delivery tasks.

A. Hardware Specification

This research utilizes a delivery robot system designed with the following hardware specifications:

1) Power Source: The primary power system consists of two 11.1V 3S Lithium Polymer (LiPo) batteries connected in series to achieve a nominal voltage of 22.2V (equivalent to a 6-cell LiPo configuration). The total capacity of the battery system is 4500 mAh.
2) Actuators: The robot is propelled by two brushed DC motors operating at a nominal voltage of 24V. These motors were selected for their stable torque output, which is essential for transporting delivery payloads.
3) Controller: An ESP32 microcontroller serves as the central data processing unit. It was chosen for its larger memory capacity, higher clock speed, and integrated WiFi module for local network communication, as well as its support for dual hardware UART serial communication for seamless Modbus integration.
4) Sensor System: A PZEM-017 DC monitoring module is employed for electrical data acquisition, paired with an external 50A / 75mV shunt resistor. Communication between the sensor and the ESP32 is established via the Modbus RTU protocol using an RS485-to-TTL converter.
5) Data Server: A personal computer running XAMPP (Apache and MySQL) serves as the local data repository, receiving and storing the electrical parameters transmitted by the ESP32 via HTTP POST requests.

B. *System Design*

The system design explains the overall structure and workflow of the delivery robot's energy monitoring system implemented in this study. Figure 1 illustrates the proposed system design.

Figure 1. System Design

Figure 1. shows the overall system design of the delivery robot's energy monitoring system. The robot is powered by two 11.1 V LiPo batteries connected in series to supply 22.2 V. A PZEM-017 sensor is used to measure voltage, current, power, and energy consumption from the battery output. The sensor data are transmitted to the ESP32 microcontroller through an RS485-to-TTL converter using UART communication. The ESP32 then sends the collected data to a local server via HTTP POST requests. A XAMPP-based server processes the data using PHP scripts and stores them in a MySQL database for monitoring and analysis.

1) Hardware Architecture

The hardware architecture is centered on the ESP32 microcontroller as the main controller. It communicates with the PZEM-017 monitoring module via a half-duplex RS485 protocol. The power source, consisting of a 22.2 V LiPo battery pack, is connected to the PZEM-017 through a 50 A/75 mV external shunt resistor, which enables accurate measurement of the high current drawn by the two brushed DC motors. The ESP32 also uses its integrated Wi-Fi module to connect to a local area network (LAN) for automated data transmission to the local server.

2) Data Acquisition and Local Logging

The software is designed to perform continuous monitoring with a specific sampling rate. As shown in the system workflow, the ESP32 initiates a Modbus request to the PZEM-017 to read the input registers. Once the raw data is retrieved, the firmware applies the necessary conversion factors and a 0.5 correction multiplier to account for the 50A shunt configuration.

The processed data (Voltage, Current, Power, and Energy) is then encapsulated into an HTTP GET request. By the data is transmitted to a local server running XAMPP. A PHP script receives the HTTP POST requests and stores the energy consumption metrics into a MySQL database structured format for post-experimental analysis

3) Electrical Design

The monitoring system is powered by two 11.1 V Lithium Polymer (LiPo) batteries connected in series to provide a 22.2 V supply, which is regulated to 5 V using a DC-DC buck converter for the ESP32 microcontroller, RS485-to-TTL converter, and PZEM-017 sensor module.

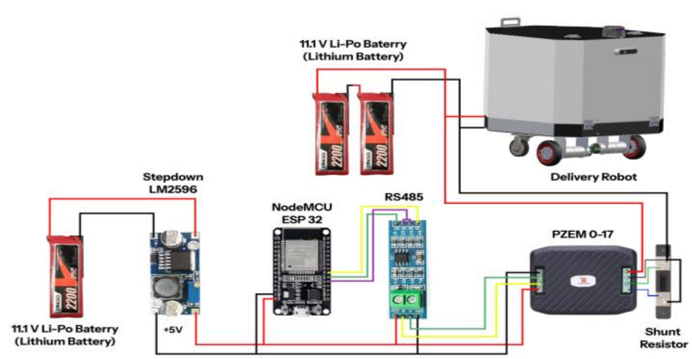

Figure 2. Electrical Design

Figure 2. illustrates the electrical design of the monitoring system. The system is powered by a dual-battery configuration consisting of two 11.1 V Lithium Polymer (LiPo) batteries connected in series to provide a 22.2 V nominal voltage. This high-voltage source is regulated to 5 V using a DC-DC buck converter to supply the ESP32 microcontroller, the RS485-to-TTL converter, and the PZEM-017 sensor module.

To enable data acquisition, the ESP32 is interfaced with the PZEM-017 through an RS485 communication module. UART communication is established using the RX2 (GPIO 16) and TX2 (GPIO 17) pins of the ESP32. A hardware optimization is applied by connecting the DE (Data Enable) and RE (Receiver Enable) pins of the RS485 module together and linking them to a single digital pin (GPIO 4) on the ESP32. This configuration simplifies the control of transmit and receive modes using a single control signal.

The physical wiring between the RS485 module and the PZEM-017 follows an A-to-A and B-to-B connection scheme. Electrical parameters of the robot, including voltage (V), current (I), and power (P), are measured through a terminal block connected to a 50 A/75 mV external shunt resistor. All components, including the ESP32, RS485 converter, and PZEM-017 sensor, are integrated into a centralized monitoring unit to ensure stable and reliable data logging.

4) Algorithm

The algorithm of the monitoring system is designed to ensure a structured and continuous data acquisition process. The overall workflow of the system is illustrated in the flowchart shown in Figure 3.

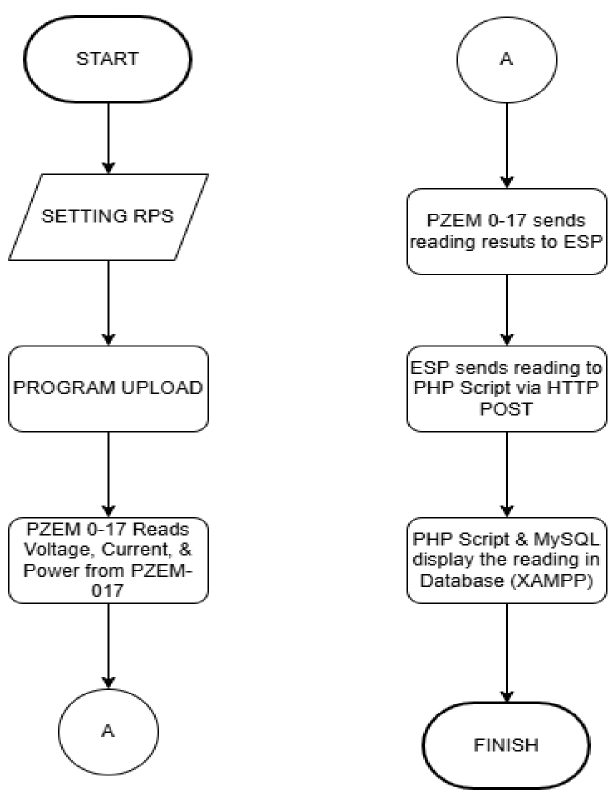

Figure 3. Flowchart system

Figure 3. illustrates the operational flow of the monitoring system. The process starts with setting the motor speed in terms of RPS (Revolutions Per Second) and uploading the program to the ESP32. After initialization, the PZEM-017 sensor measures the electrical parameters, including voltage, current, and power, from the robot's battery system.

The measured data are then transmitted to the ESP32 through the RS485 communication interface. Next, the ESP32 sends the processed readings to a PHP script using HTTP POST requests. The PHP script stores and displays the data in a MySQL database within the XAMPP environment. This process is repeated continuously to enable real-time monitoring during the robot's operation.

C. Data Acquisition and Mathematical Formulation

The PZEM-017 sensor is configured by default for a 100 A/75 mV shunt resistor. Since this study uses a 50 A/75 mV shunt, the raw data obtained from the Modbus registers are twice the actual values. Therefore, a correction factor $k = 0.5$is applied to the current, power, and energy measurements to ensure accurate results. The following equations are used to process the raw register data.

1) Voltage Calculation

The voltage value is obtained by dividing the raw register value by 100 to convert it into volts:

$$V = \frac{Reg[0x0000]}{100} \quad (1)$$

Equation (1) converts the raw voltage data from the PZEM-017 register into the actual voltage value in volts.

2) Current Calculation

The raw current data are converted from milliamperes to amperes and multiplied by the correction factor k:

$$I = \left(\frac{Reg[0x0001]}{1000}\right) \times k \quad (2)$$

Equation (2) calculates the actual current by converting the register value to amperes and compensating for the 50 A shunt resistor.

3) Power Calculation

The power value is calculated from a 32-bit register and scaled by the correction factor:

$$P = \left(\frac{RawPower}{10}\right) \times k \quad (3)$$

Equation (3) determines the real power consumption by adjusting the raw power data using the correction factor.

4) Energy Calculation

The accumulated energy value is adjusted using the correction factor:

$$E = Reg[0x0005] \times k \quad (4)$$

Equation (4) calculates the actual energy consumption in watt-hours (Wh) based on the corrected register value.

Where $k = 0.5$ is the correction factor for the 50 A/75 mV shunt resistor configuration.

D. *Energy Consumption Analysis under RPS Variations*

This subsection describes the method used to evaluate the energy consumption of the delivery robot under different motor rotational speed (RPS) conditions. The motor rotational speed was varied from 1 to 5 Revolutions Per Second (RPS), while the robot carried a constant payload of 8 kg. In this study, motor rotational speed (RPS) refers to the commanded speed level applied through the motor control system and represents relative operating speed settings rather than direct encoder-based rotational speed measurements. Each test was conducted over a fixed duration of 300 seconds (5 minutes) to ensure consistent measurement conditions.

The electrical performance analysis is based on the average voltage and current values recorded during each test interval. The electrical power consumed by the robot is calculated using the fundamental electrical power equation:

$$P = V \times I \qquad (5)$$

Equation (5) calculates the electrical power consumption, where $P$is the electrical power in Watts (W), $V$is the measured voltage in Volts (V), and $I$is the corrected current in Amperes (A). The current value is adjusted using a correction factor $k = 0.5$to compensate for the 50 A / 75 mV shunt resistor configuration during the data acquisition process on the ESP32.

The total energy consumption for each RPS level is then calculated by multiplying the average power by the measurement duration:

$$E = P \times t \qquad (6)$$

Equation (6) determines the total energy consumption, where $E$is the energy in Watt-hours (Wh) and $t$represents the test duration in hours. Since each experiment lasts 300 seconds, the time is converted as follows:

$$t = 300\ \mathrm{s} = 0.0833\ \mathrm{h}$$

The calculated power and energy consumption values for each RPS setting are summarized in Table VII and further discussed in the Results section.

E. *Battery Capacity and Usage Time Analysis*

The battery usage time of the delivery robot is determined based on the relationship between the battery capacity and the motor working current. The estimation of the operational duration is calculated using the following equation:

Battery usage time = Battery capacity / Motor working current (7)

Equation (7) defines the maximum operating time of the robot under continuous load, where the battery capacity is expressed in Ampere-hours (Ah) and the motor working current represents the average current drawn by the motors during operation.

To account for battery inefficiency, voltage drop, and safety considerations, a battery deficiency factor of 20% is applied. The battery deficiency is calculated using the following equation:

Battery deficiency = Battery capacity × 20% (8)

Equation (8) represents the additional capacity reserved to prevent deep discharge and to ensure safe and reliable battery operation.

The required battery capacity for the delivery robot is then determined by adding the deficiency value to the nominal battery capacity, as expressed by:

Required battery capacity = Battery capacity + Battery deficiency (9)

Equation (9) defines the minimum battery capacity required to support the robot's operation under maximum load conditions while maintaining battery health and system reliability.

III. RESULT AND DISCUSSION

This section presents and discusses the experimental results obtained from the electrical performance evaluation of the delivery robot under different motor rotational speed (RPS) conditions. The analysis focuses on the relationship between motor rotational speed, electrical power consumption, energy usage, and battery endurance. To ensure data stability and minimize the influence of transient current fluctuations, each RPS level ranging from 1 to 5 was tested continuously for a duration of 300 seconds (5 minutes) under a constant payload of 8 kg.Sensor Calibration and Data Validation

TABLE I.
AVERAGE OUTPUT PARAMETERS AT MOTOR ROTATIONAL SPEED OF 1 RPS (60-SECOND INTERVAL)

Time (s)	Voltage (V)	Current (A)	Power (W)	Energy (Wh)
0	24.50	1.15	28.18	0.00
60	24.42	1.15	28.08	0.47
120	24.36	1.14	27.77	0.93
180	24.29	1.15	27.93	1.40
240	24.23	1.14	27.62	1.86
300	24.15	1.15	27.77	2.32

Table I. shows the average voltage, current, power, and energy consumption of the delivery robot at 1 RPS with a 60-second sampling interval over a 300-second test duration. The results indicate stable voltage and current values, resulting in consistent power consumption and a gradual increase in accumulated energy.

TABLE II.
AVERAGE OUTPUT PARAMETERS AT MOTOR ROTATIONAL SPEED OF 2 RPS (60-SECOND INTERVAL)

Time (s)	Voltage (V)	Current (A)	Power (W)	Energy (Wh)
0	23.85	1.82	43.41	0.00
60	23.78	1.85	43.99	0.73
120	23.70	1.88	44.56	1.48
180	23.62	1.88	44.41	2.22
240	23.54	1.88	44.26	2.95
300	23.40	1.86	43.52	3.68

Table II. presents the average electrical parameters of the delivery robot at 2 RPS with a 60-second sampling interval over a 300-second duration. The results show an increase in current and power consumption compared to 1 RPS, accompanied by a steady accumulation of energy over time.

TABLE III.
AVERAGE OUTPUT PARAMETERS AT MOTOR ROTATIONAL SPEED OF 3 RPS (60-SECOND INTERVAL)

Time (s)	Voltage (V)	Current (A)	Power (W)	Energy (Wh)
0	23.42	2.55	59.72	0.00
60	23.33	2.65	61.82	01.03
120	23.23	2.70	62.72	02.07
180	23.13	2.75	63.61	3.13
240	23.03	2.80	64.48	4.21
300	22.90	2.85	65.27	5.30

Table III. shows the average electrical parameters of the delivery robot at 3 RPS with a 60-second sampling interval over a 300-second test duration. The results indicate a further increase in current and power consumption, leading to a higher rate of energy accumulation compared to lower RPS levels.

TABLE IV
AVERAGE OUTPUT PARAMETERS AT MOTOR ROTATIONAL SPEED OF 4 RPS (60-SECOND INTERVAL)

Time (s)	Voltage (V)	Current (A)	Power (W)	Energy (Wh)
0	23.25	3.42	79.51	0.00
60	23.11	3.52	81.35	1.35
120	22.97	3.59	82.46	2.72
180	22.83	3.66	83.56	4.11
240	22.69	3.73	84.64	5.52
300	22.51	3.82	85.99	6.95

Table IV. presents the average voltage, current, power, and energy consumption of the delivery robot at 4 RPS during a 300-second test. The data demonstrate a noticeable rise in power demand and energy usage as the motor speed increases.

TABLE V
AVERAGE OUTPUT PARAMETERS AT MOTOR ROTATIONAL SPEED OF 5 RPS (60-SECOND INTERVAL)

Time (s)	Voltage (V)	Current (A)	Power (W)	Energy (Wh)
0	23.10	4.25	98.18	0.00
60	22.84	4.45	101.64	1.69
120	22.54	4.58	103.23	3.41
180	22.24	4.70	104.53	5.15
240	21.94	4.82	105.74	6.91
300	21.64	4.95	107.12	8.70

Table V illustrates the electrical performance of the delivery robot at 5 RPS with a 60-second sampling interval over a 300-second duration. The highest current and power consumption are observed at this speed, resulting in the greatest accumulated energy among all tested RPS levels.

A. *Energy Consumption under RPS Variations*

This subsection presents the electrical performance of the delivery robot under different motor rotational speed (RPS) conditions, ranging from 1 to 5 RPS. During the experiments, the robot operated with a constant payload of 8 kg.

The power and energy consumption values were calculated based on the average voltage and current measurements recorded over a fixed test duration of 300 seconds (5 minutes) for each RPS level, following the methodology described in the Method section. The corresponding power and energy consumption results for each RPS variation are summarized in Table VII.

TABLE VII.
ENERGY CONSUMPTION UNDER RPS VARIATION

Motor Rotational Speed (RPS)	V (V)	I (A)	P=V×I (W)	t (h)	E=P×t (Wh)
RPS 1	24.32	1.15	27.97	833	2.33
RPS 2	23.66	1.86	44.01	833	3.67
RPS 3	23.20	2.72	63.10	833	5.26
RPS 4	22.88	3.62	82.83	833	6.90
RPS 5	22.12	4.62	102.19	833	8.51

Table VII. summarizes the calculated power and total energy consumption for each RPS level. The results show a clear increasing trend in both power demand and energy usage as the motor speed increases. At higher RPS levels, the robot draws more current, resulting in significantly greater power consumption and accumulated energy usage compared to lower speed conditions.

B. *Battery Capacity and Usage Time Analysis*

This subsection presents the battery capacity requirements and operational usage time of the delivery robot under different motor rotational speed (RPS) conditions. The analysis is based on the average current drawn by the motors at each RPS level, while the robot operates with a constant payload of 8 kg. All calculations were performed using the method described in Section E.

TABLE VIII.
BATTERY CAPACITY AND USAGE ANALYSIS

Motor Rotational Speed (RPS)	Motor Working Current (Iavg)	Battery Capacity (Ah)	Battery Deficiency (Ah)	Required Capacity (Ah)	Battery Usage Time (Hours)
RPS 1	1.15 A	4.5	0.9	5.4	3.91 (234 min)
RPS 2	1.86 A	4.5	0.9	5.4	2.41 (145 min)
RPS 3	2.74 A	4.5	0.9	5.4	1.64 (98 min)
RPS 4	3.62 A	4.5	0.9	5.4	1.24 (74 min)
RPS 5	4.63 A	4.5	0.9	5.4	0.97 (58 min)

Table VIII. summarizes the battery usage time and required battery capacity for RPS levels ranging from 1 to 5. The results show that increasing motor speed leads to higher current consumption, which directly reduces the battery usage time. At lower speeds, the robot operates with longer endurance, while higher RPS levels significantly shorten the operating duration.

Based on the results presented in Tables VII and VIII, variations in motor rotational speed (RPS) significantly influence the electrical characteristics and battery endurance of the delivery robot, even under a constant payload of 8 kg. Higher RPS levels result in increased motor working current, leading to greater power and energy consumption during operation.

Across the tested RPS range from 1 to 5, the average power consumption increases from 27.91 W to 103.50 W, with the corresponding energy consumption for a 5-minute operation rising from 2.32 Wh to 8.70 Wh. This increase in energy demand directly impacts the operational endurance of the battery system.

For a 4.5 Ah battery, the estimated operating time decreases substantially from 3.91 hours (234 minutes) at RPS 1 to 0.97 hours (58 minutes) at RPS 5. After incorporating a 20% battery deficiency factor to ensure safe operation, the required battery capacity for reliable performance across all tested conditions is determined to be 5.4 Ah.

IV. CONCLUSION

This research confirms that motor rotational speed (RPS) has a significant influence on the electrical power consumption of a delivery robot operating under a constant payload of 8 kg. The experimental results demonstrate a clear increasing trend, where raising the motor speed from 1 to 5 RPS leads to a substantial increase in average power consumption, from 27.91 W to 103.50 W.

The increase in power demand directly impacts the battery endurance of the system. Higher motor rotational speeds result in greater energy consumption and significantly reduce the operational time of the robot. For a 4.5 Ah battery system, the estimated battery usage time decreases from 234 minutes at 1 RPS to 58 minutes at 5 RPS.

Although the results provide valuable insights into the energy consumption characteristics of the delivery robot, the experiments were conducted under controlled laboratory conditions with a fixed payload. Future work should consider more realistic operating scenarios, including varying terrain profiles, dynamic load conditions, and long-term usage patterns, to further enhance battery capacity estimation and power management strategies.

REFERENCES

[1] Alfiyan, M., Puriyanto, R.D.: Mecanum 4 Omni Wheel Directional Robot Design System Using PID Method. JFSC 1(1), 6–13 (2023). https://doi.org/10.59247/jfsc.v1i1.27.

[2] Tunggal, T.P., Kirana, L.A., Arfianto, A.Z., Helmy, E.T., Waseel, F.: The Design of Ta- chometer Contact and Non-Contact Using Microcontroller. JRC 1, (2020). https://doi.org/10.18196/jrc.1315.

[3] Mukherjee, A., Misra, S., Raghuwanshi, N.S.: A survey of unmanned aerial sensing solu- tions in precision agriculture. Journal of Network and Computer Applications 148, 102461 (2019). https://doi.org/10.1016/j.jnca.2019.102461.

[4] Tagliavini, L., Colucci, G., Botta, A., Cavallone, P., Baglieri, L., Quaglia, G.: Wheeled Mo- bile Robots: State of the Art Overview and Kinematic Comparison Among Three Omnidi- rectional Locomotion Strategies. J Intell Robot Syst 106, 57 (2022). https://doi.org/10.1007/s10846-022-01745-7.

[5] Rubio, F., et al.: "Review of Mobile Robots: Concepts, Methods, Theoretical Framework, and Applications." *International Journal of Advanced Robotic Systems*, vol. 16, no. 2, pp. 1-22 (2019). https://doi.org/10.1177/1729881419839596).

[6] Millett, P.: Brushless vs. Brushed DC Motors: When and Why to Choose One Over the Other. In: 5th International Proceedings on Mechanical Engineering, pp. 1–5 (2022).

[7] Kim, J., Kim, H.: Design of Electronic Filter for Noise and Vibration Reduction in Brushed DC Motor. Machines 12(3), 148 (2024). https://doi.org/10.3390/machines12030148.

[8] Tamilselvi, S., Gunasundari, S., Karuppiah, N., Razak Rk, A., Madhusudan, S., Nagarajan, V.M., Sathish, T., Shamim, M.Z.M., Saleel, C.A., Afzal, A.: A Review on Battery Modelling Techniques. Sustainability 13(18), 10042 (2021). https://doi.org/10.3390/su131810042.

[9] Verstraten, T., Hosen, M.S., Berecibar, M., Vanderborght, B.: Selecting Suitable Battery Technologies for Untethered Robot. Energies 16(13), 4904 (2023). https://doi.org/10.3390/en16134904.

[10] Setyawan, A., et al.: "Power Consumption Analysis of Differential Drive Mobile Robot for Indoor Applications." *Journal of Robotics and Control (JRC)*, vol. 3, no. 2, pp. 145-152 (2022). https://doi.org/10.18196/jrc.v3i2.14021.

[11] Rey, A. R., & Fatekha, R. A. (2024). Analysis of battery energy consumption in the Barelang V base robot with 4 brushed DC motors. In L. Lumombo et al. (Eds.), Proceedings of the 7th International Conference on Applied Engineering (ICAE 2024) (pp. 1–20). Atlantis Press. https://doi.org/10.2991/978-94-6463-620-8_2

[12] Simanjuntak, W. P. S., & Wibisana, A. (2024). Depth camera-based human detection using YOLOv5. In Proceedings of the 7th International Conference on Applied Engineering (ICAE 2024) (pp. 150–162). Atlantis Press. https://doi.org/10.2991/978-94-6463-620-8_12

[13] Mubarak, A., Jamaaluddin, J., Anshory, I.: Implementasi Sensor Pzem-017 untuk Monitor- ing Arus, Tegangan dan Daya pada Instalasi Panel Surya dengan Sistem Data Logger Menggunakan Google Spreadsheet dan

Smartphone. In: 10th International Conference on Energy, pp. 1–10 (2022).

[14] Hung, P.D., Chin, V.V., Chinh, N.T., Tung, T.D.: A Flexible Platform for Industrial Appli- cations Based on RS485 Networks. JCM 15(3), 245–255 (2020). https://doi.org/10.12720/jcm.15.3.245-255.

[15] Prasetyo, H. E., et al.: "Real-time Battery Monitoring System for Mobile Robot Using Internet of Things (IoT) Based on Google Sheets." *Journal of Applied Engineering and Technological Science*, vol. 4, no. 1, pp. 210-218 (2022).